Reactive Component Injection Control of the Modular Multi-Output Power Electronic Transformer

Shaodi Ouyang, Jinjun Liu, Shuguang Song, Xingxing Chen
School of Electrical Engineering
Xi'an Jiaotong University
Xi'an, Shaanxi, China
Email: oysd1989@stu.xjtu.edu.cn

***Abstract*—Power Electronic Transformer(PET) is a promising component in the future power system. The modular PET is the most attractive due to its high voltage level and flexible function. Unfortunately, when the modular PET is driving multiple loads, there would be overmodulation issue in the AC-DC stage caused by the unbalanced load power. This paper proposed a reactive component injection control strategy to prevent overmodulation for a three-module PET under unbalanced load. Two specific algorithms are proposed. The effectiveness of the proposed control strategy and the two algorithms are verified by simulation results.**

I. Introduction

The power electronic transformer(PET), or solid state transformer(SST) is an emerging topic in the past decade [1].Among various topologies, the module topology, which uses cascade H bridge(CHB) as AC-DC stage and multiple DABs as DC-DC stage has become most attractive for two reasons: the CHB enables the PET to interfacing MV/HV AC grid; the multiple DABs provide various choice of connection between PET and loads which brings flexible functions[2].

One possible configuration of PET is to supply multiple loads with the modules, as shown in Fig.1. This is attractive when the loads are of different voltage rating, or the loads themselves require galvanic isolation. In recent years two PETs of such connection are published [3][4]. Unfortunately, this connection will bring unequal power issue to the CHB stage modules C when the load power is severely unequal, the CHB module power will also be severely unequal. The unequal power will cause unequal distribution of modules AC voltage which brings over-modulation issue.

In the past years, some research work on this issue has already been done on CHB converter by M. Rezaei, H.Iman-Eini, and S.Farhangi in [5], as well as on cascade PV converter by Liming Liu and Hui Li in [6][7][8], but not very complete.

[5] gives a minimum reactive current algorithm, but the operation range of that algorithm limited. In [5], this range is not studied, and no alternative algorithm is provided when the system is operating out of that range.

[6][7] proposes a reactive power sharing algorithm. In their work, two rotation frames needs to be built: a D-Q frame and a D'-Q' frame. The D axis is aligned with the grid voltage while D' axis is aligned with the grid current. Their algorithm of reactive component distribution is: the Q' axis-voltage of all the modules are set equal, meanwhile, the D' axis voltage of all the modules are set proportional to their power. This algorithm is complicated as it requires two rotational frames. What's more, the idea of sharing q' axis voltage meanwhile setting D' axis voltage proportional to their power, seems not to be the optimized.

Based on [6][7], [8] introduces a novel reactive voltage distribution method which adjusts the Q' axis component for a two-module system. The Q' axis voltages no longer needs to be equal, but re-distributed by some better coefficient. However, the method in [8] is based on a closed-loop trial and error process, but not based on a clear mathematical process. Consequently, without enough mathematical process, the derived distribution coefficient is not proved to be the optimized.

In this paper, the authors proposed a reactive component injection control strategy to handle the over-modulation issue under the unbalanced-load condition. Three specific algorithms are proposed: Shared U_D algorithm, Minimum I_Q Algorithm and the Maximum U_M Algorithm.

Although a real PET may consist of N (more than 3) modules, this paper only discusses the three-module PET as a start of this sort of research. The theory and idea in this paper form the fundamental of N module case.

The paper is organized as follows: Part II introduces the topology and the operation range under unity power factor mode; Part III introduces the basic theory of reactive component injection control; Part IV introduces three specific algorithms; Part V shows the simulation results.

II. PET AC-DC Stage Under Unity Power Factor Control

The three-module single-phase three-load PET, shown in Fig.1 is the most simple and fundamental case of single-phase multi-load PETs. The input stage is a three-module CHB rectifier; the isolation stage consists of three DAB converters.

The U/I vectors of the PET AC-DC stage with unity power factor ($i_Q^* = 0$) control is shown in Fig.2. For simplicity, the

978-1-5090-1546-7/16/$31.00 ©2016 IEEE

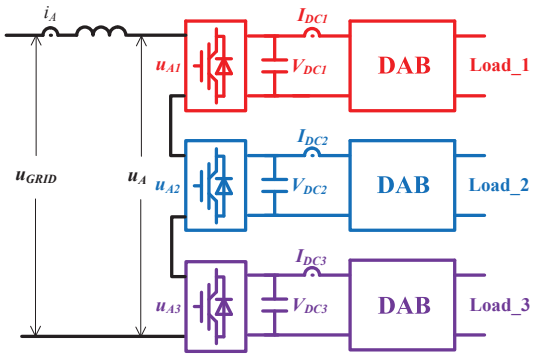

Fig. 1. Multi-Load Power Electronic Transformer

inductor voltage drop is neglected, $u_A = u_{GRID}$. The power equation is (1) and voltage equation is (2).

$$\begin{cases} P_1 = I_A \cdot U_{A1} = I_A \cdot m_{A1} \cdot V_{DC}/\sqrt{2} \\ P_2 = I_A \cdot U_{A2} = I_A \cdot m_{A2} \cdot V_{DC}/\sqrt{2} \\ P_3 = I_A \cdot U_{A1} = I_A \cdot m_{A3} \cdot V_{DC}/\sqrt{2} \end{cases} \tag{1}$$

$$U_{GRID} = U_A = U_{A1} + U_{A2} + U_{A3} \tag{2}$$

where U_{GRID} is the grid RMS voltage; I_A is the grid RMS current; U_{A1} is the module #1 AC RMS voltage, U_{A2} is the module #2 AC RMS voltage and U_{A3} is the module #3 AC RMS voltage; P_1,P_2 and P_3 are the modules' load power; m_{A1},m_{A2} and m_{A3} are the modules' modulation index.

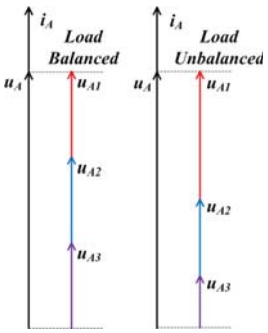

Fig. 2. U/I Vectors Under Unity Power Factor

The operation range of the system is related to another coefficient: the rated modulation index m_{rated}. m_{rated} is a pre-designed value which represents the systems DC voltage utilization rate (3). In most applications, the rated modulation is set within the range of (0.7, 0.95).The modulation indexes should not exceed 1. For simplicity, we always assume $P_1 > P_2 > P_3$ and $P_1 = 1$ in this paper. The operation range can be easily derived as (4) and can be drawn in Fig.3. The red triangle shows all possible range of unbalanced load power, and the purple region is the available region of unity power factor control.

$$U_{GRID} = 3m_{rated}V_{DC}/\sqrt{2} \tag{3}$$

$$\frac{P_2 + P_3}{P_1} > 3m_{rated} - 1 \tag{4}$$

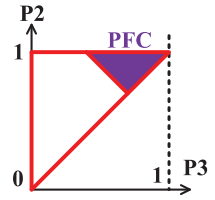

Fig. 3. Operation Range Under Unity Power Factor

III. Reactive Component Injection Control

From section II, it is seen that when the system is using PFC control, the module voltage is always forced to be proportional to the load power. There is no degree of control freedom to avoid overmodulation. In order to handle the overmodulation issue when the load is too unbalanced, the PFC has to be sacrificed. A reactive current and a reactive module voltage are introduced as new control freedoms to handle the overmodulation issue. When the reactive current and reactive module voltage are injected, the U/I vectors are then as Fig.4 and the power equation is as (5)

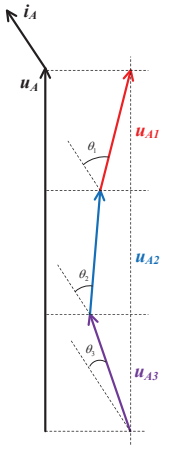

Fig. 4. U/I Vectors Under Reactive Component Injection Control

$$\begin{cases} P_1 = I_A \cdot U_{A1} \cdot cos\theta_1 \\ P_2 = I_A \cdot U_{A2} \cdot cos\theta_2 \\ P_3 = I_A \cdot U_{A3} \cdot cos\theta_3 \end{cases} \tag{5}$$

The basic idea is to increase the amplitude of grid current by injecting a reactive component. When I_A is increased, the U_{A1} will have a chance to decrease. If we let the $I_A cos\theta_1$ term in (5) be larger than the I_A term in (1), the U_{A1} will decrease thus avoiding overmodulation.

IV. Three Specific Algorithms

In this paper, three specific algorithms of the reactive component injection control strategy are proposed.

A. The Shared UD Algorithm

This subsection introduces a easy-implemented algorithmłłthe Shared U_D algorithm. Which always sets equal D-axis voltage to each module, as (6)

$$U_{D1} = U_{D2} = U_{D3} = \frac{U_{GRID}}{3} \tag{6}$$

where U_{D1}, U_{D2} and U_{A3} are the modules' D axis RMS voltage.

The reactive current is set by the following steps: 1, measure the load powers and derive the average load power as (7); 2, find the difference between each load power and the average load power, $\triangle P$, as (8); 3, set the reactive current according to (9), so the module which has the maximum $\triangle P$ will operate with a full AC output voltage, while the other two modules will generate an AC voltage smaller than full voltage, which avoids overmodulation.

$$P_{AVR} = \frac{P_1 + P_2 + P_3}{3} \tag{7}$$

$$\triangle P_k = P_k - P_{AVR} \qquad k = 1, 2, 3 \tag{8}$$

$$I_Q = \frac{\max(|\triangle P_1|, |\triangle P_2|, |\triangle P_3|)}{\sqrt{\frac{V_{DC}^2}{2} - (\frac{1}{3}U_{GRID})^2}} \tag{9}$$

The control block diagram is shown in Fig.5. It should be noted that, there are two methods to achieve DC voltage balancing: the first method is just as Fig.5 shows, by setting D axis voltage at 1/3 for each module while trimming the Q axis voltage through a DC voltage balancing loop; the second method, in contrast, is to set the Q axis voltage by some mathematical calculation while trimming the D axis voltage through a DC voltage balancing loop. Both the two methods will lead to a same final steady state result. Comparing these two methods, the first one is easier implemented; the second one is a little more complicated, but it tends to have a better performance in cases when I_Q is too small to achieve DC voltage balancing.

The Shared U_D algorithm is full-range available, which is an advantage over the two other algorithms in the latter part.

B. The Minimum IQ Algorithm

The Minimum I_Q Algorithm always ensure u_{A1} be in phase with i_A meanwhile $m_{A1} = 1$. At certain P_1,P_2 and P_3($P_1 > P_2 > P_3$), this can ensure a minimum reactive current as well as a minimum overall current. The algorithm is as (10).

Note that (10) only determines i_Q, U_{D1} and U_{Q1}. The AC reference for the other two modules, u_2 and u_3, are generated by a DC voltage balancing loop in the latter part of this subsection.

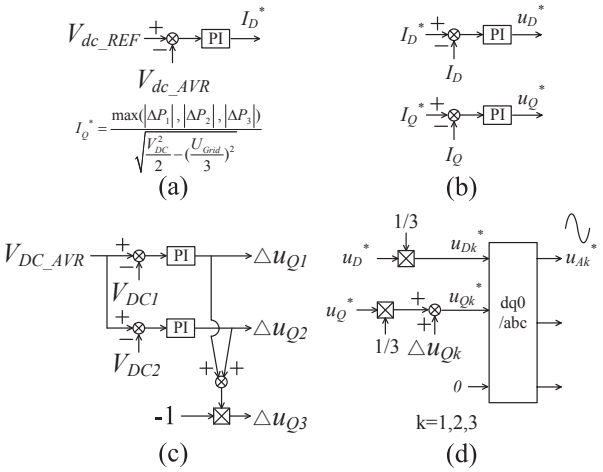

Fig. 5. Control Blocks of Shared UD Algorithm

$$\begin{cases} U_{D1} = \dfrac{I_D V_{DC}^2}{2P_1} = \dfrac{(1 + \frac{P_2+P_3}{P_1})V_{DC}^2}{2U_{GRID}} \\ U_{Q1} = \sqrt{\dfrac{V_{DC}^2}{2} - U_{D1}^2} \\ I_Q = \dfrac{P_1 - U_{D1} I_D}{\sqrt{\frac{V_{DC}^2}{2} - V_{D1}^2}} \\ U_{D2} + U_{D3} = U_{GRID} - U_{D1} \\ U_{Q2} + U_{Q3} = -U_{Q2} \end{cases} \tag{10}$$

The available range of Minimum I_Q Algorithm is derived by a geometric approach which summarizes all possible position and length of u_{A1}, u_{A2} and u_{A3} vectors.

The u_{A1}, u_{A2} and u_{A3} vectors have to meet several constraints. Firstly, the sum of all three modules' AC voltages should be equal to the grid voltage (11). It can also be written in form of modulation index (12).

$$u_{A1} + u_{A2} + u_{A3} = u_{GRID} \tag{11}$$

$$m_{A1} + m_{A2} + m_{A3} = 3m_{rated} \tag{12}$$

Secondly, the u_{A1} is full in amplitude, that is (13)

$$m_{A1} = 1 \tag{13}$$

Thirdly, the other two modules' AC voltages should not exceed full amplitude (14)

$$\begin{cases} m_{A2} \leq 1 \\ m_{A3} \leq 1 \end{cases} \tag{14}$$

With these constraints, the operation range can be derived by Fig.6. θ is the angle between u_{A1} and u_{GRID}. Under different θ, the maximum component of u_{A2} on the direction of u_{A1}, as well as the minimum component of u_{A3} on the direction of u_{A1} can be found. As long as they are found, the upper

limit of P_2 and the lower limit of P_3 under different θ are also found, then the available range of Minimum I_Q Algorithm can be derived.

As the θ turns bigger, the boundary cases are shown in Fig.6(a)-(e).

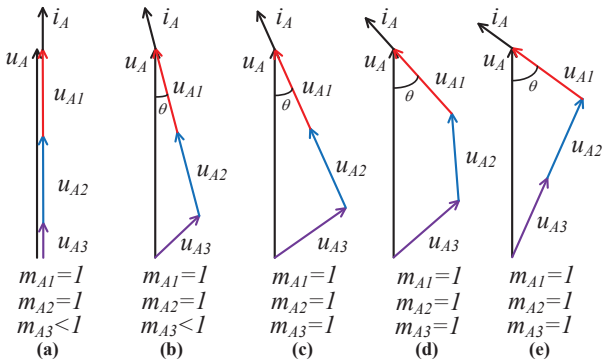

Fig. 6. Boundary U/I Vectors of Minimum IQ Algorithm

Fig.6(a) shows the PFC case. In PFC case, P_2 can be maximized by setting $m_{A2} = 1$ meanwhile making u_{A2} in phase with u_{A1}.

Fig.6(b) shows a reactive component injection case. In this case, u_{A2} can still be set at $m_{A2} = 1$ meanwhile in phase with u_{A1}. As the θ is within a certain limit, $m_{A3} < 1$ is ensured. In this case, the upper limit of P_2 and the lower limit of P_3 is as (15)

$$\begin{cases} P_2 + P_3 = 3cos(m_{rated}) - 1 \\ P_{2\_MAX} = 1 \\ P_{3\_MIN} = 3cos(m_{rated}) - 2 \end{cases} \tag{15}$$

Fig.6(c) shows the critical point of the Fig.6(b) case. In Fig.6(c), the u_{A2} can still be set at full modulation index meanwhile in phase with u_{A1}, $P_{2\_MAX} = P_1$. At the same time, the u_{A3} also reaches full amplitude, $m_{A3} = 1$. The vectors: $3m_{rated}$, 2 and 1, can form a closed triangle.

Fig.6(d) shows the case when θ exceeds the case in Fig.6(c). The maximum P_2 can be obtained by setting u_{A2} at full modulation index, but no longer able to be in phase u_{A1}. In this case, the vectors form a quadrilateral whose side lengths are: $3m_{rated}$, 1, 1 and 1. The upper limit of P_2 and the lower limit of P_3 is as (16).

$$\begin{cases} P_2 + P_3 = 3m_{rated}cos(\theta) - 1 \\ P_{2\_MAX} = \dfrac{3m_{rated}cos(\theta) - 1}{2} + \\ \dfrac{\sqrt{3 - 9m_{rated}^2 + 6m_{rated}cos(\theta)}}{\sqrt{1 + 9m_{rated}^2 - 6m_{rated}cos(\theta)}} \cdot \dfrac{3m_{rated}sin(\theta)}{2} \\ P_{3\_MIN} = \dfrac{3m_{rated}cos(\theta) - 1}{2} - \\ \dfrac{\sqrt{3 - 9m_{rated}^2 + 6m_{rated}cos(\theta)}}{\sqrt{1 + 9m_{rated}^2 - 6m_{rated}cos(\theta)}} \cdot \dfrac{3m_{rated}sin(\theta)}{2} \end{cases} \tag{16}$$

Fig.6(e) shows the critical point of Fig.6(d). In this case, the u_{A2} and u_{A3} are synchronized so the quadrilateral in Fig.6(d) goes to a triangle again, whose side lengths are $3m_{rated}$, 1 and 2.

The θ can not go bigger than Fig.6(e), otherwise the vectors will not be able to form a closed polygon.

Summarizing all the results from Fig.6,(15) and (16), the available range of Minimum I_Q Algorithm can be drawn in Fig.7 as the blue line surrounded area.

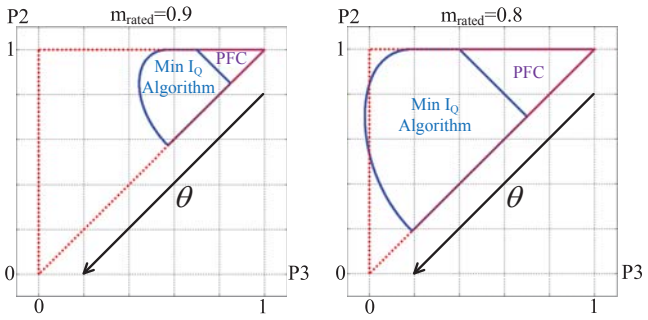

Fig. 7. Operation Range Under Minimum IQ Algorithm

The control implementation is a little complicated. The I_Q^* is given by (10). U_{D1} is given by (10) while U_{D1} is given by its own DC voltage loop, as in Fig.8. Again, here we could also set U_{Q1} according to (10) while letting U_{D1} be given by the DC voltage loop.

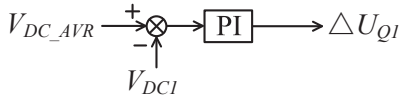

Fig. 8. VDC1 Control Loop

The DC balancing loop of #2 and #3 has two forms according to different θ.

When θ is small, the location of operating point will locate in region A as Fig.9(a) shows. In region A, the trajectory of u_{A2} and u_{A3} is shown in Fig.9(b). When the system in working at M1 point where $P_2 = P_3$, the u_{A2} and u_{A3} will be the same at $\frac{u_A - u_{A1}}{2}$. When the system is working at M2 point where P_2 reaches the maximum value while P_3 reaches the minimum value, the u_{A2} and u_{A3} will be as Fig.6(b), where $m_{A2} = 1$ and u_{A2} be in phase with u_{A1}, meanwhile $m_{A3} < 1$. Therefore, the adjustment direction should be chosen as the green arrow, which is $u_{A1} - \frac{u_A - u_{A1}}{2}$. The balancing loop is shown by Fig.10 and (17).

When θ is big, the location of operating point will locate in region B as Fig.9(a) shows. In region B, the trajectory of u_{A2} and u_{A3} is shown in Fig.9(c). When the system in working at N1 point where $P_2 = P_3$, the u_{A2} and u_{A3} will be the same at $\frac{u_A - u_{A1}}{2}$. When the system is working at N2 point where P_2 reaches the maximum value while P_3 reaches the minimum value, the u_{A2} and u_{A3} will be as Fig.6(d), where $m_{A2} = m_{A3} = 1$. Therefore, the adjustment direction should

be chosen as the green arrow, which is vertical to $u_A - u_{A1}$. The balancing loop is shown by Fig.10 and (18).

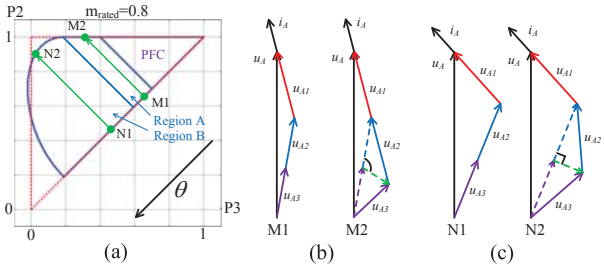

Fig. 9. U/I Vectors Under Minimum IQ Algorithm

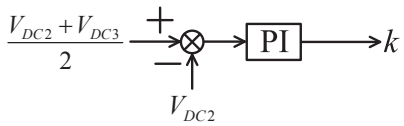

Fig. 10. VDC2 and VDC3 Control Loop

$$\begin{cases} u_{A2} = \dfrac{u_A - u_{A1}}{2} + k \cdot \dfrac{u_{A1} - \frac{u_A - u_{A1}}{2}}{\left| u_{A1} - \frac{u_A - u_{A1}}{2} \right|} \\ u_{A3} = u_A - u_{A1} - u_{A2} \end{cases} \tag{17}$$

$$\begin{cases} u_{A2} = \dfrac{u_A - u_{A1}}{2} + k \cdot \perp \left(\dfrac{u_A - u_{A1}}{|u_A - u_{A1}|} \right) \\ u_{A3} = u_A - u_{A1} - u_{A2} \end{cases} \tag{18}$$

C. The Maximum UM Algorithm

As have stated above, the Minimum I_Q Algorithm is unable to cover all the required region. Therefore, a Maximum U_M Algorithm is proposed for the uncovered region.

The region is derived through the following logical process:

1, At the boundary of Minimum I_Q Algorithm region, there is always $m_{A1} = m_{A2} = m_{A3} = 1$ and i_A be in phase with u_{A1}. Like J1 and K1 in Fig.11.

2, Starting from the Minimum I_Q Algorithm boundary, if the voltage vectors are kept while the reactive current is increased, the system operating point will cover all the region which is uncovered by the Minimum I_Q Algorithm. As an example, if the system starts from J1(K1), by adding reactive current, the system operating point will move through J2(K2) to J3(K3), like Fig.11 and Fig.12 shows.

It is straightforward seen that, by setting $m_{A1} = m_{A2} = m_{A3} = 1$, the required I_Q must be the minimized value. Otherwise, if the I_Q continues to decrease, the modules will have to increase their AC voltages to maintain the power, which results in overmodulation. As this algorithm features $m_{A1} = m_{A2} = m_{A3} = 1$, it is called the Maximum U_M Algorithm

The control objective of this method is to ensure $m_{A1} = m_{A2} = m_{A3} = 1$. The key loops are shown in Fig.13.

Fig.13(a) is the DC voltage balancing loop, which ensures $V_{DC1} = V_{DC2} = V_{DC3}$;

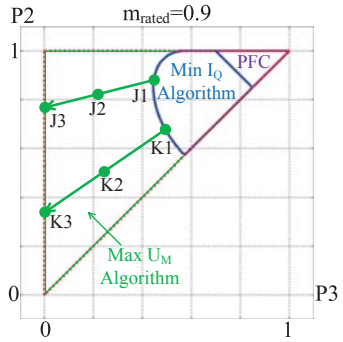

Fig. 11. Operation Range of Maximum UM Algorithm

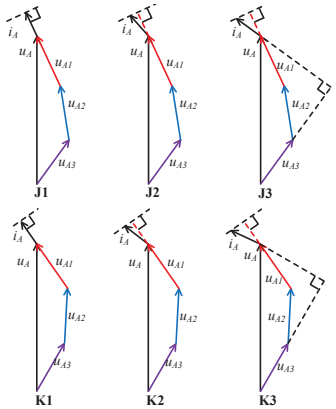

Fig. 12. U/I Vectors of J1/J2/J3 and K1/K2/K3 points in Fig.11

Fig.13(b) is the AC voltage amplitude(U_M) balancing loop, or the modulation index balancing loop. If one module's AC voltage amplitude is smaller than the average, it will increase its D axis voltage. The reason why D axis voltage is able to adjust the AC voltage amplitude can be found in Fig.14. As the Maximum U_M Algorithm is derived by adding extra reactive component to the Minimum I_Q Algorithm, the angle of i_A will always be larger than all the module AC voltages, thus the terminal location of the AC voltages are all to the right side of i_A like Fig.14 shows. When a module power is constant, the location of its AC voltage vector terminal will be restricted on the corresponding red line which is vertical to i_A. It is easily obtained that, when the voltage vector terminal moves on its corresponding red line, a larger U_D(as well as a larger U_Q) always corresponds to a larger U_M. Therefore, U_M can be adjusted by U_D(or U_Q).

This loop will ensure $m_1 = m_2 = m_3 = m_{AVR}$.

Just like what is stated in Shared U_D algorithm, here we could also exchange the use of U_Q and U_D: using U_D for DC voltage balancing while U_Q for modulation index balancing, and it would lead to a same final control result.

Fig.13(c) is the I_Q adjusting loop. The I_Q will be adjusted according to the modules' average AC voltage amplitude. If m_{AVR} is smaller than 1, it will indicate that the modules' AC voltage capacity is not fully utilized, then the I_Q can be decreased. This loop will ensure $m_{AVR} = 1$.

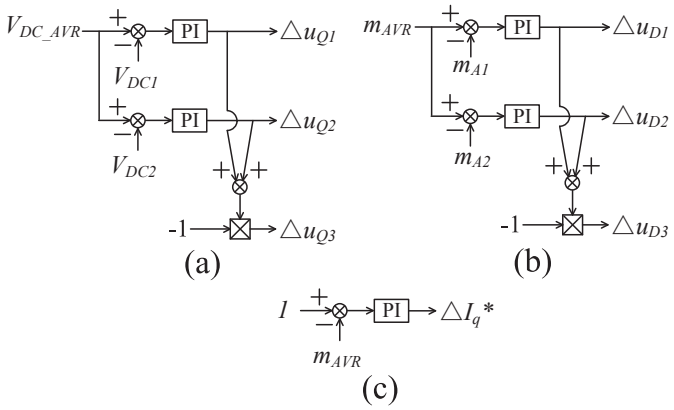

Fig. 13. Control Loops of Maximum UM Algorithm

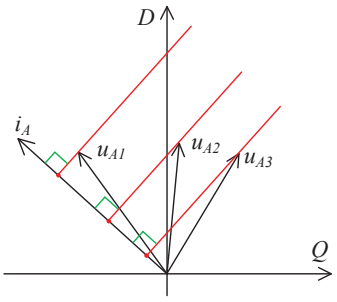

Fig. 14. The Explanation of UM Balancing Loop

V. Simulation Results

In order to verify the proposed reactive component injection control, simulation is carried out in SIMULINK. A single phase three-module PET is built. The parameters of PET AC-DC stage are shown in TABLE I. The DAB stage parameters and waveforms will not be shown because the DAB stage is not concerned in this paper.

TABLE.1 PET AC-DC Stage Parameters

Grid Voltage	220V(RMS)
Module Number	3
Rated Power	1500W(Each Module)
DC voltage	130V
m_{rated}	0.8
Switching Frequency	10kHz(Each Module)
Inductor	1mH

In order to verify all the three algorithms, two sets of simulation are done. The operating points are marked in Fig.15.

A. P1:P2:P3=1:0.8:0.2

$P_1 : P_2 : P_3 = 1 : 0.8 : 0.2$, this point is located within the available area of Minimum I_Q Algorithm. Two algorithms are used to control the system, the Shared U_D algorithm and the Minimum I_Q Algorithm, then the outputs are compared.

Fig.16 shows the grid voltage/current and the modulation waves under Shared U_D algorithm. As $P_1 : P_2 : P_3 = 1 : 0.8 : 0.2$, there is $|\triangle P_3| > |\triangle P_1| > |\triangle P_2|$, according to the theory of Shared U_D algorithm, the control result should be $1 = m_{A3} > m_{A1} > m_{A2}$. This results is verified by the waves.

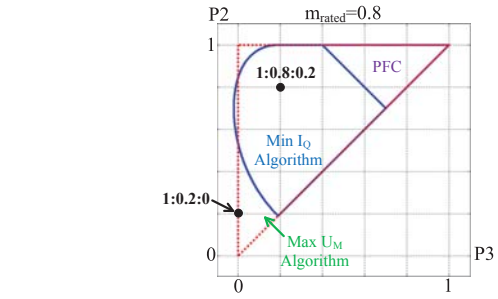

Fig. 15. Two Simulated Points

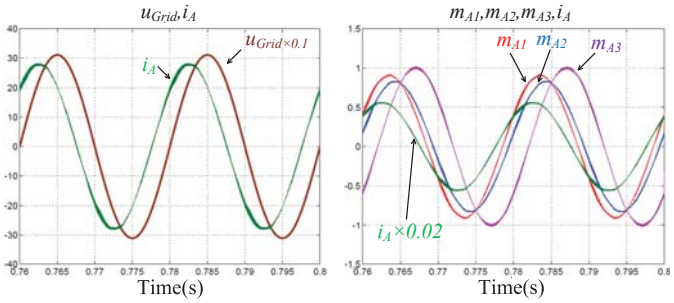

Fig. 16. P1:P2:P3=1:0.8:0.2 under Shared UD Algorithm

Fig.17 shows the grid voltage/current and the modulation waves under Minimum I_Q algorithm. According to the theory of Minimum I_Q algorithm, the control result should be $m_{A1} = 1$ and u_{A1} be in phase with i_A. This results is verified by the waves.

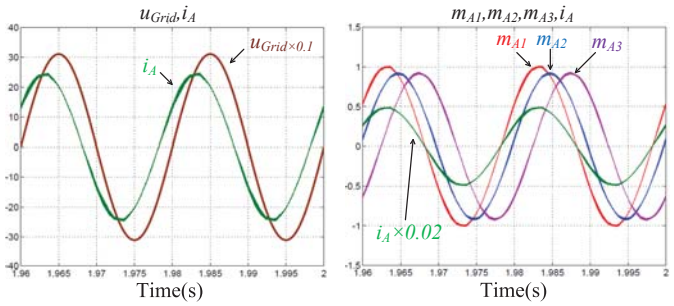

Fig. 17. P1:P2:P3=1:0.8:0.2 under Minimum IQ Algorithm

The current amplitude of Fig.17 is smaller than that of Fig.16, which proves that the Minimum I_Q algorithm requires the smallest I_Q as well as the smallest current amplitude.

B. P1:P2:P3=1:0.2:0

$P_1 : P_2 : P_3 = 1 : 0.2 : 0$, this point is located outside of the available area of Minimum I_Q Algorithm. Two algorithms

are used to control the system, the Shared U_D algorithm and the Maximum U_M Algorithm, then the outputs are compared.

Fig.18 shows the grid voltage/current and the modulation waves under Shared U_D algorithm. As $P_1 : P_2 : P_3 = 1 : 0.2 : 0$, there is $|\triangle P_1| > |\triangle P_3| > |\triangle P_2|$, according to the theory of Shared U_D algorithm, the control result should be $1 = m_{A1} > m_{A3} > m_{A2}$. This results is verified by the waves.

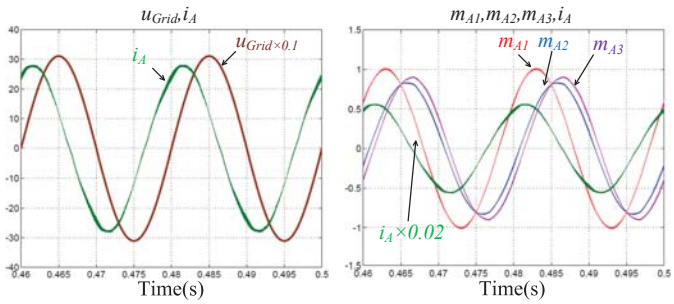

Fig. 18. P1:P2:P3=1:0.2:0 under Shared UD Algorithm

Fig.19 shows the grid voltage/current and the modulation waves under Maximum U_M algorithm. According to the theory of Maximum U_M algorithm, the control result should be $m_{A1} = m_{A2} = mA3 = 1$. This results is verified by the waves.

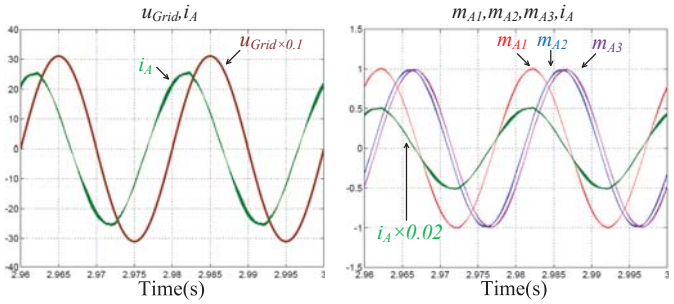

Fig. 19. P1:P2:P3=1:0.2:0 under Maximum UM Algorithm

The current amplitude of Fig.19 is also smaller than that of Fig.18, which proves that the Maximum U_M algorithm also requires the smallest I_Q as well as the smallest current amplitude.

VI. Conclusion

This paper proposes a reactive component injection control strategy to handle the over-modulation issue for the AC-DC stage of multi-output PET. In a modular multi-output PET, the AC-DC stage module power is determined by the load power. When the load power is unbalanced, the AC-DC stage module power, as well as the module AC voltage, will also be unbalanced. If the system just applies unity power factor (iQ*=0) control, overmodulation will occur.

In order to handle the overmodulation issue, this paper proposed a reactive component injection control to eliminate the overmodulation issue. Including three specific algorithms: the Shared U_D algorithm , Minimum I_Q Algorithm and the Maximum U_U Algorithm. The basic theory of these algorithms are discussed and their control blocks are shown.

Comparing the three algorithms, the Shared U_D algorithm is easy implemented and full-range available, but it requires larger reactive current; the Minimum I_Q algorithm and Maximum U_M Algorithm are comparably complicated, only partial-range available, but they can minimize the required reactive current.

The proposed reactive component injection control and its three algorithms are verified by simulation results.

References

[1] Johann W. Kolar, Gabriel Ortiz. "Solid-State-Transformers: Key Components of Future Traction and Smart Grid Systems", In Proc. IEEE Power Electronics Conference (IPEC-Hiroshima 2014 - ECCE-ASIA), 2014.

[2] Xu She, Xunwei Yu, Fei Wang and Alex Q. Huang. Design and Demonstration of a 3.6-kVC120-V/10-kVA Solid-State Transformer for Smart Grid Application, IEEE Transactions on Power Electronics, vol.29, no.8, 2014.

[3] Xinyu Wang, Jinjun Liu, Shaodi Ouyang, Fei Meng. "Research on Unbalanced-Load Correction Capability of Two Power Electronic Transformer Topologies", IEEE Transactions on Power Electronics, vol.30, no.6, 2015.

[4] Michail Vasiladiotis, Alfred Rufer, "A Modular Multiport Power Electronic Transformer With Integrated Split Battery Energy Storage for Versatile Ultrafast EV Charging Stations", IEEE Transactions on Industrial Electronics, vol.62, no.5, 2015.

[5] M. Rezaei, H. Iman-Eini, and S. Farhangi, Grid-connected photovoltaic system based on a cascaded H-Bridge inverter, J. Power Electron.,vol. 12, no. 4, 2012.

[6] L. Liu, H. Li, and Y. Xue, "control strategy for grid-connected cascaded photovoltaic (PV) system in high voltage high power applications, in Proc. IEEE APEC, 2013.

[7] Liming Liu, Hui Li, Yaosuo Xue and Wenxin Liu, Decoupled Active and Reactive Power Control for Large-Scale Grid-Connected Photovoltaic Systems Using Cascaded Modular Multilevel Converters, IEEE Trans. on Power Electronics, Vol.30, No.1, 2015.

[8] Liming Liu, Hui Li, Yaosuo Xue, and Wenxin Liu. "Reactive Power Compensation and Optimization Strategy for Grid-Interactive Cascaded Photovoltaic Systems", IEEE Transactions on Power Electronics, vol.30, no.1, 2015.